

# ROBUST $H_{\infty}$ OPTIMAL CONTROLLER DESIGN FOR THE SMALL UNMANNED AERIAL VEHICLE

**Róbert SZABOLCSI**

*Óbuda University, Budapest, Hungary*  
 szabolcsi.robert@bgk.uni-obuda.hu

## ABSTRACT

*This article deals with robust  $H_{\infty}$  optimal control of the flight control systems of the small unmanned aerial vehicles (UAVs) in the presence of the plant disturbances and sensor noises. The rationales of the theory of  $H_{\infty}$  controller synthesis are brought into a unique frame supporting design procedures being implemented. The paper focuses on numerical example of the synthesis of the controller of the flight control system of the small UAV.*

**KEYWORDS:** UAV, modelling, automatic flight control system, dynamic optimal control,  $H_{\infty}$  design

## 1. Introduction

The UAV flight automation is an emerging problem due to flight safety aspects. In order to design reliable and safe automatic flight control systems many factors must be taken account. Flight safety itself represents the critical point of the UAS design both in flight and ground maintenance of the UAV. Secondly, integration of the UAV into airspaces being used is very important and serves as key element recently. The UAV has today very wide range of applications, and, it is widening day by day.

The UAV automatic flight control systems must be able handle critical flight situations, and, must be able to ensure robustness in the meaning of the external disturbance rejection ability and sensor noise attenuation feature of the closed loop flight control systems.

Robustness of the closed loop flight control system is a minimum standard applicable in design of the plant controllers. The motive of this research is to design

robust controller for the small UAV ensuring dynamic performances defined for the closed loop flight control system, and to present a design example of the proposed  $H_{\infty}$  design.

## 2. Preliminaries and Literature Review

The control system analysis and design leaning on traditional classical control theory are duly demonstrated in numerous references (Shahian and Hassul, 1993; Ogata, 1999; Burns, 2001; Franklin and Powell, 2002; Stefani, Savant and Hostetter, 2002). McLean (1990), Szabolcsi (2011, 2016), Chingiz and Vural (2013), Zulu and John (2014), Bokor, Gáspár and Szabó (2014), Lee, Lee, Yoo, Moon and Tahk (2014), Aliyu, Chindo and Opasina (2015), and finally, Fessi and Bouall`egue (2016) solved numerous modern control engineering problems in the field of the UAV automatic flight control systems using LQR and LQG controller synthesis methods.

The problems related to formulation of the  $H_\infty$  controller design are well-known since many decades. In early works of Maciejowski (1989) and Grimble (1994) basics for robust control system design had been elaborated, and, finally it has been solved in 2006 by Apkarian, P.

After, many software applications were available inside MATLAB to support solution of the design problem (MATLAB 9.5, R2018b).

UAV flight automation is an emerging problem due to flight safety aspects. In order to design reliable and safe automatic flight control systems disturbances and noises must be considered in controller synthesis (Chingiz & Vural, 2013; Zulu & John, 2014; Lee, Lee, Yoo, Moon & Tahk, 2014; Aliyu, Chindo &

Opasina, 2015). The UAV closed loop flight control system dynamic performances being implemented are elaborated by R. Szabolcsi (2015, 2016). The solution of the numerical example of this article is supported by MATLAB R2018b supplemented with Control System Toolbox (2018) and Robust Control Toolbox (2018).

### 3. The Rationals – The Optimal Control Problem Formulation

The two input/two output (TITO) representation of the augmented multivariable system can be seen in Figure no. 1. (Apkarian, 2006; Bokor, Gáspár & Szabó, 2014).

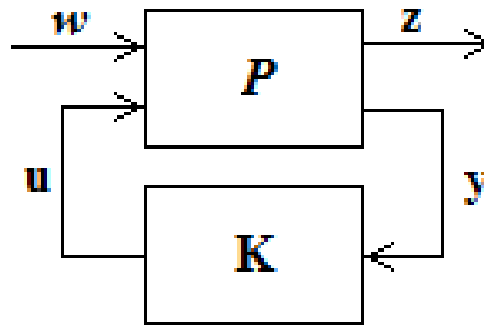


Figure no. 1: Block diagram of the TITO-system

where  $P(s)$  is the plant to be controlled,  $K(s)$  is the stabilizing controller,  $u$  is the control input vector,  $w$  is the vector of the exogenous inputs (fixed commands, unknown commands, disturbances, noises),  $z$  is the regulated output, and, finally,  $y$  is the measured output vector.

The  $H_\infty$  optimal control problem can be formulated as follows: for the given plant dynamics of  $P(s)$  compute the optimal state space controller of  $K^*(s)$  of the original  $K(s)$  controller such that (Apkarian, 2006; Bokor, Gáspár & Szabó, 2014):

$$\left\{ \begin{array}{l} \min \|T_{w \rightarrow z}(P, K)\|_\infty \\ \text{subjected to } K \text{ stabilizes } P \text{ internally} \\ \text{and } K \in \mathcal{K} \end{array} \right\} \quad (1)$$

where in equation (1) the  $H_\infty$ -norm of the closed loop performance channel is represented by  $T_{w \rightarrow z}(P, K)$ . Easy to agree

that the controller synthesis means choice of the proper controller space denoted by  $\mathcal{K}$ .

The augmented plant dynamics  $P(s)$  space model: can be represented by the following state

$$\left. \begin{aligned} \dot{\mathbf{x}}(t) &= \mathbf{A}\mathbf{x}(t) + \mathbf{B}_1\mathbf{w}(t) + \mathbf{B}_2\mathbf{u}(t) \\ \mathbf{z}(t) &= \mathbf{C}_1\mathbf{x}(t) + \mathbf{D}_{11}\mathbf{w}(t) + \mathbf{D}_{12}\mathbf{u}(t) \\ \mathbf{y}(t) &= \mathbf{C}_2\mathbf{x}(t) + \mathbf{D}_{21}\mathbf{w}(t) + \mathbf{D}_{22}\mathbf{u}(t) \end{aligned} \right\} \quad (2)$$

or, using standard matrix notation:

$$\text{TITO}(s) : \begin{bmatrix} \dot{\mathbf{x}} \\ \mathbf{z} \\ \mathbf{y} \end{bmatrix} = \begin{bmatrix} \mathbf{A} & | & \mathbf{B}_1 & \mathbf{B}_2 \\ \hline \mathbf{C}_1 & | & \mathbf{D}_{11} & \mathbf{D}_{12} \\ \mathbf{C}_2 & | & \mathbf{D}_{21} & \mathbf{D}_{22} \end{bmatrix} \begin{bmatrix} \mathbf{x} \\ \mathbf{w} \\ \mathbf{u} \end{bmatrix} = \mathbf{P}(s) \begin{bmatrix} \mathbf{x} \\ \mathbf{w} \\ \mathbf{u} \end{bmatrix} \quad (3)$$

where

$$\mathbf{P}(s) = \begin{bmatrix} \mathbf{A} & | & \mathbf{B}_1 & \mathbf{B}_2 \\ \hline \mathbf{C}_1 & | & \mathbf{D}_{11} & \mathbf{D}_{12} \\ \mathbf{C}_2 & | & \mathbf{D}_{21} & \mathbf{D}_{22} \end{bmatrix}, \quad (4)$$

$\mathbf{x} \in \mathbb{R}^{n_p}$  is the state vector,  $\mathbf{u} \in \mathbb{R}^{n_u}$  is the control input vector,  $\mathbf{y} \in \mathbb{R}^{n_y}$  is the measured output vector,  $\mathbf{w} \in \mathbb{R}^{n_w}$  is the

exogenous input vector,  $\mathbf{z} \in \mathbb{R}^{n_z}$  is the regulated output vector.

The state space controller  $\mathbf{K}(s)$  in Figure no. 1 can be represented as given below:

$$\mathbf{K}(s) : \begin{cases} \dot{\mathbf{x}}_K = \mathbf{A}_K\mathbf{x}_K + \mathbf{B}_K\mathbf{y} \\ \mathbf{u} = \mathbf{C}_K\mathbf{x}_K + \mathbf{D}_K\mathbf{y} \end{cases} \quad \mathbf{K}(s) : \begin{bmatrix} \mathbf{A}_K & | & \mathbf{B}_K \\ \hline \mathbf{C}_K & | & \mathbf{D}_K \end{bmatrix} \quad (5)$$

with  $\mathbf{x}_K \in \mathbb{R}^k$  the state of  $\mathbf{K}$ .

The closed loop transfer channel of  $\mathbf{T}_{w \rightarrow z}(\mathbf{P}, \mathbf{K})$  in equation (1) will have the

following state space representation that (Apkarian, 2006):

$$\mathbf{T}_{w \rightarrow z}(\mathbf{P}, \mathbf{K}) : \begin{bmatrix} \mathbf{A}(\mathbf{K}) & | & \mathbf{B}(\mathbf{K}) \\ \hline \mathbf{C}(\mathbf{K}) & | & \mathbf{D}(\mathbf{K}) \end{bmatrix} \quad (6)$$

where the state dimension is  $n_p + k$ .

The  $H_\infty$ -norm of equation (1) is defined as:

$$\|\mathbf{T}_{w \rightarrow z}(\mathbf{P}, \mathbf{K})\|_\infty = \max_{\omega \in \mathbb{R}} \bar{\sigma}(\mathbf{T}(j\omega)) \quad (7)$$

where notation  $\bar{\sigma}(\mathbf{M})$  represents the maximum singular value of the complex matrix  $\mathbf{M}$ .

If to close the loop in Figure no. 2, one may consider that the closed-loop control system as a linear operator of  $T_{w \rightarrow z}(P, K)$  mapping input vector  $w$  to the output vector of  $z$ .

If the controller  $K(s)$  stabilizes internally the plant  $P(s)$ , in other words,  $A(K)$  in equation (6) is stable one, then operator of  $T_{w \rightarrow z}(P, K)$  maps  $w \in \mathcal{L}^2$  into  $z \in \mathcal{L}^2$ , and, the  $H_\infty$ -norm in equation (7) is the  $\mathcal{L}^2$ - $\mathcal{L}^2$  operator, thus, we have:

$$\|T_{w \rightarrow z}(P, K)\|_\infty = \sup_{\omega \neq 0} \frac{\|T\omega\|_2}{\|\omega\|_2} = \sup_{\omega \neq 0} \frac{\|z\|_2}{\|w\|_2} \quad (8)$$

Equation (8) derives for the closed-loop system channel  $w \rightarrow z$  the norm of  $\gamma = T_{w \rightarrow z}(P, K)$ , which is a factor by which input signal energy is amplified in the system output  $z$ . Input signal  $w$  of the system with energy of  $\|w\|_2^2$  will produce output signal of

$z$  with energy  $\|z\|_2^2$  being no greater than  $\gamma^2 \cdot \|w\|_2^2$  as closed loop controller  $K$  is used. The optimization strategy defined by equation (1) tries to find stabilizing controller  $K(s)$  for which the amplification factor of  $\gamma$  is the smallest, i.e.:

$$\|z\|_2 \leq \gamma^2 \cdot \|w\|_2, \quad \text{where } \gamma = \|T_{w \rightarrow z}(P, K)\|_\infty \quad (9)$$

This representation is very useful because all one has to do is to find channel  $w \rightarrow z$ , and, the smallness of the system output  $z$  to the closed loop system input  $w$  tells us more about the closed loop control

system. This idea is widely used in loop shaping of the closed loop control systems depicted in Figure no. 2 (Apkarian, 2006; Bokor, Gáspár & Szabó, 2014).

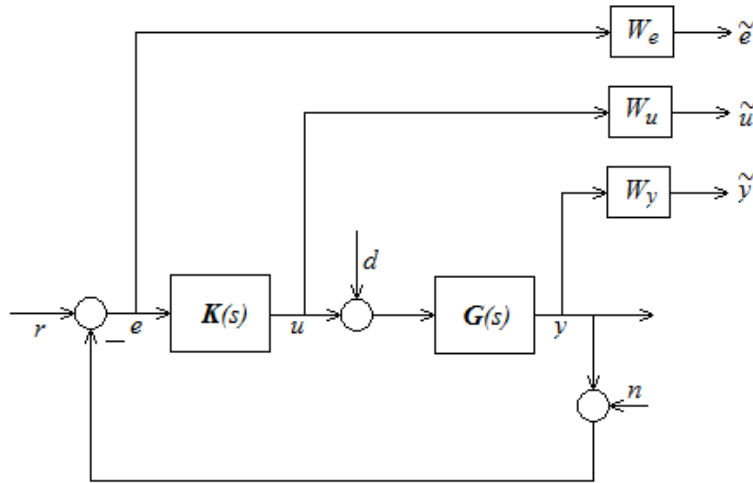


Figure no. 2: The standard loop shaping of the closed loop control system

The closed loop control system scheme shown in Figure no. 2 features the open loop system dynamics  $G(s)$ , the controller  $K(s)$ , the measured output  $y$ , the control vector  $u$ , and the tracking error  $e$ . The system inputs are reference signal  $r$ , external disturbance or plant noise  $d$ , and finally, sensor noise  $n$ . The

closed loop control system's chosen outputs are  $\tilde{e} = W_e e$ ,  $\tilde{u} = W_u u$ , and  $\tilde{y} = W_y y$ . In this case the input vector  $w^T = [r \ d \ n]$ , and the output vector is  $z^T = [\tilde{e} \ \tilde{u} \ \tilde{y}]$ , where filters are modeled with  $W_e$ ,  $W_u$ , and  $W_y$ . The filters introduced in Figure no. 2 may be static or dynamic ones. If they are

dynamic, they will add new states to the plant  $P(s)$  states defined by equation (4).

For closed loop control system depicted in Figure no. 2 it is a typical dynamic performance how fast the closed loop control system is able to follow the

reference input  $r$ , and if so, what is the tracking error  $e$ . From Figure no. 2 it is evident that transfer from the reference input  $r$  to the tracking error  $e$  can be found as:

$$T_{r \rightarrow e}(K) = \frac{1}{I + G(s)K(s)} \quad (10)$$

If the tracking problem is defined for the reference signal  $r$  varying typically in the low frequency range, i.e.  $W_e$  represents a

low-pass filter. In this case the smallness of the second norm of

$$\|T_{r \rightarrow e}(K)\|_{\infty} = \left\| \frac{W_e}{I + G(s)K(s)} \right\|_{\infty} \quad (11)$$

defines how the low frequency component  $\bar{e}$  of the tracking error  $e$  is small, or, in other words, how the measured output  $y$  follows the reference input  $r$  in low frequency domain.

If to evaluate and to find influence of the sensor noise  $n$  on control signal  $u$ , the following performance channel must be set up:

$$T_{n \rightarrow \bar{u}}(K) = - \frac{K(s)}{I + G(s)K(s)} W_u \quad (12)$$

Sensor noises are typically of high frequency, however, it may never lead to high frequency components of the control vector  $u$ . It means, that  $W_u$  represents the high-pass filter, i.e.  $\bar{u}$  is the high-frequency component of the control vector  $u$ . The infinite norm of

$$\|T_{n \rightarrow \bar{u}}(K)\|_{\infty} \quad (13)$$

is putting a cost upon high-frequency components of the control vector  $u$ .

evaluate after the closed loop control system properties.

If the criteria set by equation (1) allows calculate the optimal controller  $K$  minimizing the cost, the controller design yields to robust system able to eliminate, or minimize sensor noise effects.

#### 4. A Numerical Example for the Small UAVH<sub>∞</sub>-Optimal Control System Design

Summing up preliminaries using equations (10)-(13), and from Figure no. 2 it is evident that there are many performances and robustness channels available for use to design controller, and

The UAV spatial motion can be modelled using MIMO, or SISO-approach. The MIMO dynamical model of the aircraft is given by McLean (1990). The Boomerang-60 Trainer small UAV lateral/directional motion MIMO dynamical model is given by Szabolcsi, R. (2016) and is as follows:

$$\dot{\mathbf{x}} = \begin{bmatrix} \dot{v} \\ \dot{p} \\ \dot{r} \\ \dot{\gamma} \end{bmatrix} = \mathbf{Ax} + \mathbf{Bu}$$

$$= \begin{bmatrix} -0,7724 & 0 & -18,9671 & 9,0867 \\ 1,9247 & -19,9149 & 7,7565 & 0,0000 \\ 69,1314 & -23,8689 & -2,5966 & 0,0000 \\ 0,0000 & 1,0000 & 0,0000 & 0,0000 \end{bmatrix} \begin{bmatrix} v \\ p \\ r \\ \gamma \end{bmatrix} + \begin{bmatrix} 0,0000 & 2,2582 \\ -23,8289 & 1,5015 \\ -11,7532 & -15,2855 \\ 0 & 0 \end{bmatrix} \begin{bmatrix} \delta_\alpha \\ \delta_r \end{bmatrix} \quad (14)$$

where  $v$  is the lateral speed,  $p$  is the roll rate,  $r$  is the yaw rate,  $\gamma$  is the roll angle,  $\delta_\alpha$  is the aileron angular deflection,  $\delta_r$  is the rudder angular deflection, respectively. The single

degree-of-freedom approximation of the UAV rolling motion can be deduced from equation (22) to be (Szabolcsi, 2016):

$$\dot{p}(t) = -19,9149 p(t) - 23,8289 \delta_\alpha(t) \quad (15)$$

The transfer function of the Boomerang-60 UAV is as follows:

$$Y(s) = \frac{p(s)}{-\delta_\alpha(s)} = \frac{23,8289}{s + 19,9149} = \frac{A}{1 + sT} \quad (16)$$

where  $A=1,1965$ ,  $T=0,0502$  s.

The roll rate stability augmentation system is often serves as inner loop in the roll

angle stabilization of the UAV, and it can be seen in Figure no. 3.

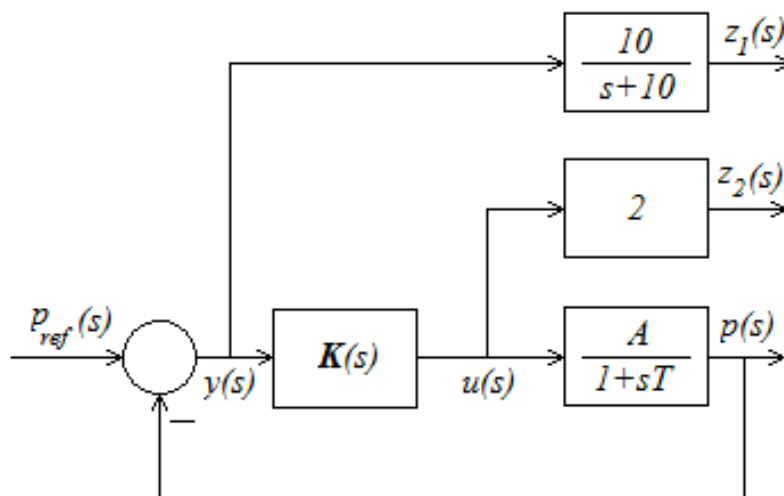


Figure no. 3: The standard loop shaping of the closed loop control system

The corresponding plant equations are as follows:

$$\left. \begin{aligned} p_{rsf} &= w \\ p &= x_1 \\ x_2 &= 0,1z_1 \rightarrow z_1 = 10x_2 \\ \dot{x}_1 &= -\frac{1}{T}x_1 + \frac{A}{T}u \\ \dot{x}_2 &= -x_1 - 10x_2 + w \\ z_2 &= 2u \\ y &= -x_1 + w \end{aligned} \right\} \quad (17)$$

Using equation (17) the plant matrices defined by equation (4) can be derived as follows:

$$\left. \begin{aligned} \mathbf{A} &= \begin{bmatrix} -\frac{1}{T} & 0 \\ -1 & -10 \end{bmatrix}; \mathbf{B}_1 = \begin{bmatrix} 0 \\ 1 \end{bmatrix}; \mathbf{B}_2 = \begin{bmatrix} \frac{A}{T} \\ 0 \end{bmatrix} \\ \mathbf{C}_1 &= \begin{bmatrix} 0 & 10 \\ 0 & 0 \end{bmatrix}; \mathbf{C}_2 = [-1 \quad 0] \\ \mathbf{D}_{11} &= \begin{bmatrix} 0 \\ 0 \end{bmatrix}; \mathbf{D}_{12} = \begin{bmatrix} 0 \\ 2 \end{bmatrix}; \mathbf{D}_{21} = 1; \mathbf{D}_{22} = 0 \end{aligned} \right\} \quad (18)$$

The optimal  $H_\infty$  state space controller  $\mathbf{K}(s)$  has been designed using MATLAB R2018b (MATLAB 2018; MATLAB Robust Control Toolbox, 2018) and its toolboxes via minimizing the closed loop control system stable transfer matrix  $\mathbf{T}_{wz_1}$  using integral performance index defined by equation (8). The *h2syn.m* embedded function of MATLAB Robust Control Toolbox will find the followings:

$\mathbf{K} - H_\infty$  controller;  
 $\mathbf{CL} = \text{lft}(\mathbf{P}, \mathbf{K})$  – LTI closed loop control system transfer function  $\mathbf{T}_{wz_1}$ ;  
 $\text{Gam} = \text{norm}(\mathbf{CL})$  –  $H_\infty$  optimal cost  $\gamma = \|\mathbf{T}_{wz_1}\|_\infty$ .

Results of the  $H_\infty$  optimal controller synthesis are as follows below:

$$\left. \begin{aligned} \mathbf{K} &= \left[ \begin{array}{c|c} \mathbf{A}_k & \mathbf{B}_k \\ \hline \mathbf{C}_k & \mathbf{D}_k \end{array} \right] \\ \mathbf{A}_k &= \begin{bmatrix} -19,91 & 0 \\ -1 & -10 \end{bmatrix}; \mathbf{B}_k = \begin{bmatrix} 0 & 23,83 \\ 1 & 0 \end{bmatrix}; \mathbf{C}_k = \begin{bmatrix} 0 & 10 \\ 0 & 0 \\ -1 & 0 \end{bmatrix}; \mathbf{D}_k = \begin{bmatrix} 0 & 0 \\ 0 & 2 \\ 1 & 0 \end{bmatrix} \end{aligned} \right\} \quad (19)$$

$$CL = \left. \begin{array}{c} \left[ \begin{array}{c|c} A_{cl} & B_{cl} \\ \hline C_{cl} & D_{cl} \end{array} \right] \\ A_{cl} = \begin{bmatrix} -19,91 & 0 & -5,632 & 90,71 \\ -1 & -10 & 0 & 0 \\ 0 & 0 & -25,07 & 83,1 \\ -0,9161 & 0 & 0 & -10 \end{bmatrix} \\ B_{cl} = \begin{bmatrix} 0 \\ 1 \\ 0 \\ 0,9161 \end{bmatrix}; C_{cl} = \begin{bmatrix} 0 & 10 & 0 & 0 \\ 0 & 0 & -0,4727 & 7,613 \end{bmatrix}; D_{cl} = \begin{bmatrix} 0 \\ 0 \end{bmatrix} \end{array} \right\} \quad (20)$$

$$\gamma = \|T_{wz_1}\|_{\infty} = 0,8591 \quad (21)$$

The small UAV roll rate stability augmentation system has been tested in time domain (Szabolcsi, 2011, 2014, 2016;

MATLAB 2018). Results of the computer simulation can be seen in Figure no. 3.

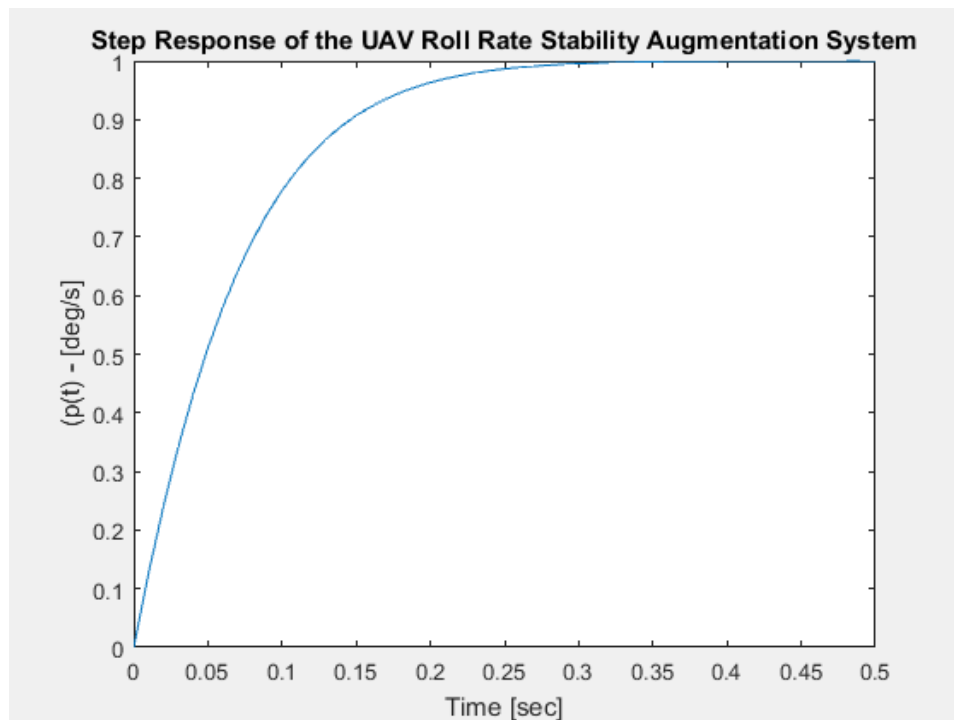


Figure no. 4: Result of the time domain analysis of the closed loop control system.

From Figure no. 4 it is easy to determine that UAV closed loop roll rate stability augmentation system has very fast response to the unit step change in the roll rate. Regarding system of the criteria set in

(15, 16) there is no overshoot in the normalized step response. In other words, the entire closed loop automatic flight control system of the small UAV behaves with non-oscillatory feature.

## 5. Conclusions

The motive behind this research work was to solve the  $H_\infty$  design problem in the field of controller synthesis for the small UAV disturbed by external disturbances and sensor noises, too.

The  $H_\infty$  design procedure is widely applied in flight control of the UAV, and, it supports to ensure robustness of the closed loop flight control system via minimizing

second norm of the chosen robustness measure.

The rationale to this UAV control problem has been set up, and a numerical solution to a given robust controller synthesis problem has been demonstrated. The robust controller will ensure closed loop control system dynamic performances defined well-advanced.

## REFERENCES

- Aliyu, B. K., Chindo, A. M., Opasina, A. O., & Abdulrahman, A. (2015) Comparative Design for Improved LQG Control of Longitudinal Flight Dynamics of a Fixed-Wing UAV. *Advances in Research*, 3(5), 477-487.
- Apkarian, P., & Noll, D. (2006). Nonsmooth  $H_\infty$ -synthesis. *IEEE Transactions on Automatic Control*, Vol. 51, No.1, 229-244.
- Bokor, J., Gáspár, P., & Szabó, Z. (2014). *Modern Control Engineering*. Budapest: Budapest University of Technology and Economics.
- Burns, R. S. (2001) *Advanced Control Engineering*. Oxford-Auckland-Boston-Johannesburg-Melbourne-New Delhi: Butterworth-Heinemann.
- Chingiz, H., & Vural, S.Y. (2013). LQR Controller with Kalman Estimator Applied to UAV Longitudinal Dynamics. *Scientific Research*, Vol. 4, 36-41.
- Fessi, R., & Bouallegue, S. (2016). Modeling and Optimal LQG Controller Design for a Quadrotor UAV, *3<sup>rd</sup> International Conference on Automation, Control, Engineering and Computer Science (ACECS'16)*, 264-270.
- Franklin, G. F., Powell, J. D., & Emami-Naeini, A (2002). *Feedback Control of Dynamic Systems*. Reading – Menlo Park – New York – Don Mills – Wokingham – Amsterdam – Bonn – Sydney – Singapore – Tokyo – Madrid – San Juan – Milan – Paris: Addison-Wesley Publishing Company.
- Grimble, M. J. (1994). *Robust Industrial Control Optimal - Design Approach for Polynomial Systems*. New York: Wiley.
- H. Lee, H., Lee, B., Yoo, D., Moon, G., & Tahk, M. (2014). Dynamics Modeling and Robust Controller Design of the Multi-UAV Transportation System. *29<sup>th</sup> Congress of the ICAS, St. Petersburg*, 7-12 September.
- Maciejowski, M. (1989). *Multivariable Feedback Design*. London, UK: Addison-Wesley Publishing Company.
- MathWorks. (2018). *MATLAB<sup>®</sup> Control System Designer/Control System Toolbox 10.3, User's Guide*, MA: Author.
- MathWorks. (2018). *MATLAB<sup>®</sup> R2018b, User's Guide*. MA: Author.
- MathWorks. (2018). *MATLAB<sup>®</sup> Robust Control Toolbox, User's Guide*. MA: Author.
- McLean, D. (1990). *Automatic Flight Control Systems*. New York – London – Toronto – Sydney – Tokyo – Singapore: Prentice-Hall International Ltd.
- Ogata, K. (1999). *Modern Control Engineering*, New York – London: Prentice-Hall.
- Shahian, B., & Hassul, M. (1993) *Control System Design Using MATLAB<sup>®</sup>*. Englewood Cliffs, New Jersey: Prentice-Hall.

Stefani, R. T., Shahian, B., Savant Jr., C.J., & Hostetter, G. H. (2002) *Design of Feedback Control Systems*: Oxford University Press, New York-Oxford.

Szabolcsi, R. (2011). *Computer Aided Design of Modern Control Systems*. Budapest: Miklós Zrínyi National Defense University.

Szabolcsi, R. (2014). Lateral/Directional Flying Qualities Applied in UAV Airworthiness Certification Process. *Land Forces Academy Review*, 3(75), 336-346.

Szabolcsi, R. (2014). UAV Longitudinal Motion Flying Qualities Applied in Airworthiness Certification Procedure. *Land Forces Academy Review*, 2(74), 208-216.

Szabolcsi, R. (2016). *Automatic Flight Control of the UAV*. Budapest: Óbuda University.

Zulu, A., & John, S. (2014). A Review of Control Algorithms for Autonomous Quadrotors. *Open Journal of Applied Sciences*, 4, 547-556.